Bulletin of the Earthquake
Research Institute
Vol. 43 (1965), pp. 291-316

20. *A Long Wave in the Vicinity of an Estuary [I]* —*An Analysis by the Method of the Buffer Domain*—.

By Takao Momoi,

Earthquake Research Institute.

(Read March 23, 1965.—Received March 31, 1965.)

Abstract

In this paper, a long wave in the vicinity of an estuary is treated by use of the method of the buffer domain.

Dividing the whole domain into three parts, the equation of a long wave is solved analytically by use of the Fourier Bessel expansion. Then an electronic computer was used to obtain the wave heights and phases in each domain. The conclusions obtained in the present purview are:—

(1) For the waves propagating into the canal, when kd (k: the wave number of the incident waves; d: half the width of the canal) approaches to zero, the wave height tends to double that of the incident waves, the phase becomes zero and the waves in the canal are propagated as if they originated at an infinite point. When kd increases in amount, the wave height diminishes monotonically to reach that of the incident waves at about $kd=1.0$, the phase takes a maximum value at about $kd=0.3$ and later decreases monotonically to zero value at $kd=1.0$, and the supposed origin of the waves propagated into the canal approaches the estuary.

(2) For the waves in front of the mouth of the canal, the equi-amplitude and phase lines run parallel to the coast facing the open sea and the amplitude of the waves increases in the direction of the offing. Provided that the linear approximations for sine and cosine functions are possible, it is found that the waves in front of the mouth of the canal are propagated with the speed of a long wave into the canal.

(3) As far as the waves in the open sea are concerned, our greatest interest is in damping reflected waves (instead of merely reflected waves). Regarding these waves, the following facts are known.

When kd is small, the amplitude of the damping reflected waves is also small. As kd becomes large, a contribution of these waves to reflected waves is augmented. For the rates of the damping of

these waves versus a variation of position, a similar tendency is seen. That is to say, the damping rate is gentle for small kd and rapid for large kd. And the rate is remarkable, in magnitude, in the surrounding part of the mouth of the canal.

The surface composed by the amplitudes of the damping reflected waves tends to an asymptotic surface as kd becomes large.

Finally, concerning the directivity of the damping reflected waves, the fact is known that a contribution of these waves to reflected ones is small in the direction along the coast and becomes large as a line, along which a variation of the damping reflected waves is examined, is directed to the offing.

1. Introduction

When the Chilean Tsunami of 1960 attacked Japan, severe damage was incurred in the surrounding parts of the estuaries. Such heavy inundations are considered to be due to the following two reasons: (1) the nearby part of the estuary is low in land topography and (2) the tsunami waves are diffracted into the rivers or canals around the estuary. The second possibility mentioned above has not yet been examined, hence it is checked in this article. Besides this examination, the behaviors of the waves in the vicinity of the estuary are scrutinized also in the present purview. The analysis has been carried out by use of the method of the buffer domain, which was first developed by the author. For this method, readers should refer to a paper under the title "The Method of the Buffer Domain in the Water with a Step Bottom".[1)]

In Section 2, the general theory is developed without any approximation.

In Section 3, the general theory derived in Section 2 is approximated to obtain knowledge of the waves in nearby areas of a mouth of the canal.

2. General Theory

Referring to Fig. 1, the origin of the coordinates is located in the center of the mouth of the canal, the x- and y-axes being taken along the coastline and in the sense of the banks of the canal. Let the

1) T. MOMOI, *Bull. Earthq. Res. Inst.*, **41** (1965), 296. In Section 2 of this paper, the method of the buffer domain was outlined.

domains separate into three parts as shown in Fig. 1, i. e.,

D_1: the domain in the range ($|x|<d$, $y<0$);

D_2: the domain in the range ($r<d$, $0<\theta<\pi$), where (r, θ) are the polar coordinates and D_2 corresponds to the "buffer domain" in the method of the buffer domain;

D_3: the domain in the range ($r>d$, $0<\theta<\pi$).

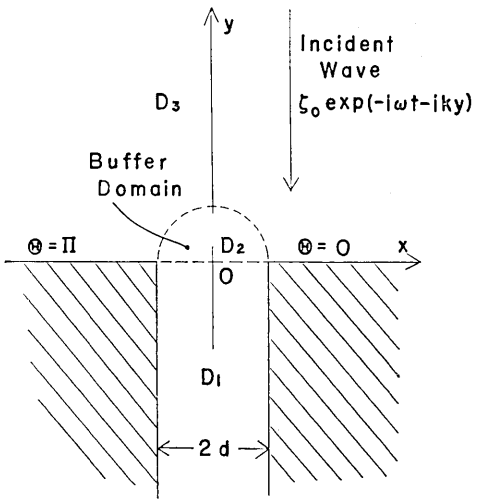

Fig. 1. A model of an estuary.

Then the basic equations for a train of the periodic waves are

$$\left(\frac{\partial^2}{\partial x^2}+\frac{\partial^2}{\partial y^2}+k^2\right)\zeta_j=0 \quad (j=1, 2, 3), \tag{1}$$

where ζ_j: the wave heights in the domains D_j;

k: the wave number of the surging waves, which is related to an angular frequency ω and the velocity c of the long wave such as

$$\omega=kc\ .$$

The conditions at the rigid boundaries are:
in the domain D_1,

$$\frac{\partial\zeta_1}{\partial x}=0 \qquad \text{at } (|x|=d,\ y<0); \tag{2}$$

in the domain D_3,

$$\frac{\partial \zeta_3}{\partial y}=0 \qquad \text{at } (|x|>d,\ y=0)\,. \tag{3}$$

The conditions for connecting three domains with each other are:

$$\left.\begin{aligned} &\zeta_1=\zeta_2\,, \\ &\frac{\partial \zeta_1}{\partial y}=\frac{\partial \zeta_2}{\partial y}\,, \end{aligned}\right\} \text{ at } (|x|<d,\ y=0)\,, \tag{4}$$

and

$$\left.\begin{aligned} &\zeta_2=\zeta_3\,, \\ &\frac{\partial \zeta_2}{\partial r}=\frac{\partial \zeta_3}{\partial r}\,, \end{aligned}\right\} \text{ at } (r=d,\ 0<\theta<\pi)\,. \tag{5}$$

Provided that the surging periodic waves are given by

$$\zeta_0 \exp(-i\omega t-iky)\,,$$

where ζ_0 is the amplitude of the surging waves, the solution of (1) in the domain D_3 satisfying the condition (3) is given as follows:

$$\zeta_3=2\zeta_0 \cos ky+\sum_{n=0}^{\infty} \zeta_3^{(2n)} \cos 2n\theta \cdot H_{2n}^{(1)}(kr)\,, \tag{6}$$

where the first term of the above expression stands for the standing wave due to the reflection of the incident waves at the straight coast and the second group of terms denotes the scattering of the waves by the estuary, of which the azimuthal components are selected so as to satisfy the boundary condition (3). Using the Bessel expression of cosine,[2] i. e.,

$$\cos ky=\sum_{n=0}^{\infty} \varepsilon_n \cos 2n\theta \cdot J_{2n}(kr)\,, \tag{6'}$$

the expression (6) becomes

$$\begin{aligned} \zeta_3=&2\zeta_0 \sum_{n=0}^{\infty} \varepsilon_n \cos 2n\theta \cdot J_{2n}(kr) \\ &+\sum_{n=0}^{\infty} \zeta_3^{(2n)} \cos 2n\theta \cdot H_{2n}^{(1)}(kr)\,, \end{aligned} \tag{7}$$

2) G. N. WATSON, *Theory of Bessel Functions* (Cambridge, 1922).

where

$$\varepsilon_0=1 \text{ and } \varepsilon_n=2 \ (n\geqq 1) .$$

Likewise, by use of the polar co-ordinates, the solution of the equation (1) in the domain D_2 is given as follows:

$$\zeta_2=\sum_{n=0}^{\infty}\{\bar{\zeta}_2^{(2n)}\cos 2n\theta\cdot J_{2n}(kr) + \zeta_2^{(2n+1)}\sin(2n+1)\theta\cdot J_{2n+1}(kr)\} . \tag{8}$$

In the expressions (7) and (8), the azimuthal modes are taken in such a way that the symmetry of the phenomenon with respect to the y-axis is satisfied, and $\zeta_3^{(2n)}$, $\bar{\zeta}_2^{(2n)}$ and $\zeta_2^{(2n+1)}$ are the arbitrary constants to be determined by the conditions communicating the domains D_1, D_2 and D_3.

Next, following the same procedure as in the previous study for the canal[3], the solution of (1) in the domain D_1 satisfying the condition (2) becomes as follows (using the symmetry):—

$$\zeta_1=\sum_{m=0}^{\infty}\zeta_1^{(m)}\cos\frac{m\pi}{d}x\cdot e^{-ik_1^{(m)}y} , \tag{9}$$

where $\zeta_1^{(m)}$ is the arbitrary constant and

$$k_1^{(m)}=\sqrt{k^2-\left(\frac{m\pi}{d}\right)^2} .$$

In the expressions (7), (8) and (9), a time factor $\exp(-i\omega t)$ is omitted as usual (this convention is followed in the subsequent discussions, unless otherwise stated).

In order to determine the arbitrary constants in the expressions (7), (8) and (9), we have four available conditions (4) and (5).

Sustituting (8) and (9) into (4), we have:

$$\left.\begin{aligned}&\sum_{n=0}^{\infty}\bar{\zeta}_2^{(2n)}\cdot J_{2n}(kr)=\sum_{m=0}^{\infty}\zeta_1^{(m)}\cos\frac{m\pi}{d}x ,\\ &\sum_{n=0}^{\infty}\zeta_2^{(2n+1)}\cdot(2n+1)\cdot\frac{J_{2n+1}(kr)}{r}\\ &\qquad=\sum_{m=0}^{\infty}\zeta_1^{(m)}(-ik_1^{(m)})\cos\frac{m\pi}{d}x .\end{aligned}\right\} \tag{10}$$

3) T. MOMOI, *Bull. Earthq. Res. Inst.*, **40** (1962), 719.

In derivation of the latter of the relation (10), the reductions

$$\left.\begin{aligned} \frac{\partial}{\partial y}&=\frac{1}{r}\frac{\partial}{\partial\theta} \quad \text{for } \theta=0\ , \\ \frac{\partial}{\partial y}&=-\frac{1}{r}\frac{\partial}{\partial\theta} \quad \text{for } \theta=\pi\ , \end{aligned}\right\}$$

are used.

Likewise, substituting (7) and (8) into (5), we have

$$\left.\begin{aligned} &\sum_{n=0}^{\infty}\{\bar{\zeta}_2^{(2n)}\cos 2n\theta\cdot J_{2n}(kd) \\ &\quad+\zeta_2^{(2n+1)}\sin(2n+1)\theta\cdot J_{2n+1}(kd)\} \\ &=2\zeta_0\sum_{n=0}^{\infty}\varepsilon_n\cos 2n\theta\cdot J_{2n}(kd) \\ &\quad+\sum_{n=0}^{\infty}\zeta_3^{(2n)}\cos 2n\theta\cdot H_{2n}^{(1)}(kd)\ , \\ &\sum_{n=0}^{\infty}\{\bar{\zeta}_2^{(2n)}\cos 2n\theta\cdot J'_{2n}(kd) \\ &\quad+\zeta_2^{(2n+1)}\sin(2n+1)\theta\cdot J'_{2n+1}(kd)\} \\ &=2\zeta_0\sum_{n=0}^{\infty}\varepsilon_n\cos 2n\theta\cdot J'_{2n}(kd) \\ &\quad+\sum_{n=0}^{\infty}\zeta_3^{(2n)}\cos 2n\theta\cdot H_{2n}^{(1)\prime}(kd)\ . \end{aligned}\right\} \tag{11}$$

Applying the operators (one of the reductions in the method of the buffer domain):

$$\int_{-d}^{+d}\cos\frac{m\pi}{d}x\,dx \quad (m=0,1,2,\cdots)$$

and

$$\int_0^{\pi}\cos 2n\theta\,d\theta \qquad (n=0,1,2,\cdots)$$

to (10) and (11) respectively, the following infinite simultaneous equations are obtained:

$$\left.\begin{aligned} &\sum_{n=0}^{\infty}I(J_{2n},0)\cdot\bar{\zeta}_2^{(2n)}-kd\cdot\zeta_1^{(0)}=0, \\ &\sum_{n=0}^{\infty}I(J_{2n},m)\cdot\bar{\zeta}_2^{(2n)}-\frac{kd}{2}\cdot\zeta_1^{(m)}=0 \\ &\qquad\qquad(m=1,2,3,\cdots)\ , \end{aligned}\right\} \tag{12}$$

$$\left.\begin{aligned}
&\sum_{n=0}^{\infty} I\left(\frac{J_{2n+1}}{r},\ 0\right)\cdot\zeta_2^{(2n+1)}+i\cdot kd\cdot\zeta_1^{(0)}=0\ ,\\
&\sum_{n=0}^{\infty} I\left(\frac{J_{2n+1}}{r},\ m\right)\cdot\zeta_2^{(2n+1)}+i\cdot\frac{1}{2}k_1^{(m)}d\cdot\zeta_1^{(m)}=0\\
&\qquad\qquad (m=1,\ 2,\ 3,\ \cdots)\ ,
\end{aligned}\right\} \tag{13}$$

$$\left.\begin{aligned}
&J_0(kd)\cdot\overline{\zeta}_2^{(0)}+\sum_{n=0}^{\infty}\frac{2}{\pi}\frac{1}{2n+1}\cdot J_{2n+1}(kd)\cdot\zeta_2^{(2n+1)}\\
&\quad=H_0^{(1)}(kd)\cdot\zeta_3^{(0)}+2J_0(kd)\cdot\zeta_0\\
&J_{2m}(kd)\cdot\overline{\zeta}_2^{(2m)}+\sum_{n=0}^{\infty}\frac{4}{\pi}\cdot\frac{(2n+1)J_{2n+1}(kd)}{(2n+1)^2-(2m)^2}\cdot\zeta_2^{(2n+1)}\\
&\quad=H_{2m}^{(1)}(kd)\cdot\zeta_3^{(2m)}+4J_{2m}(kd)\cdot\zeta_0\\
&\qquad\qquad (m=1,\ 2,\ 3,\ \cdots)\ ,
\end{aligned}\right\} \tag{14}$$

$$\left.\begin{aligned}
&J_0'(kd)\cdot\overline{\zeta}_2^{(0)}+\sum_{n=0}^{\infty}\frac{2}{\pi}\frac{1}{2n+1}\cdot J_{2n+1}'(kd)\cdot\zeta_2^{(2n+1)}\\
&\quad=H_0^{(1)\prime}(kd)\cdot\zeta_3^{(0)}+2J_0'(kd)\cdot\zeta_0\ ,\\
&J_{2m}'(kd)\cdot\overline{\zeta}_2^{(2m)}+\sum_{n=0}^{\infty}\frac{4}{\pi}\cdot\frac{(2n+1)J_{2n+1}'(kd)}{(2n+1)^2-(2m)^2}\cdot\zeta_2^{(2n+1)}\\
&\quad=H_{2m}^{(1)\prime}(kd)\cdot\zeta_3^{(2m)}+4J_{2m}'(kd)\cdot\zeta_0\\
&\qquad\qquad (m=1,\ 2,\ 3,\ \cdots)\ ,
\end{aligned}\right\} \tag{15}$$

where

$$\left.\begin{aligned}
&I(J_{2n},\ q)=\int_0^{kd}J_{2n}(z)\cos\frac{q\pi}{kd}z\,dz\ ,\\
&I\left(\frac{J_{2n+1}}{r},\ q\right)=(2n+1)\int_0^{kd}\frac{J_{2n+1}(z)}{z}\cos\frac{q\pi}{kd}z\,dz\ ,\\
&\qquad\qquad (n,\ q=0,\ 1,\ 2,\ \cdots)
\end{aligned}\right\} \tag{16}$$

When the calculation is made, the above-mentioned simultaneous equations are solved as a finite number of simultaneous equations as usual. In the following sections, the actual calculation and the discussion of the result are made.

3. First Approximation

In order to solve the equations (12) to (15), the approximation is given to the expressions of the buffer domain. When kd is so small, the Bessel functions can be approximated such that

$$\left.\begin{aligned} &J_0(z)\simeq 1\ , \\ &J_1(z)\simeq\frac{z}{2}\ , \\ &J_m(z)\simeq 0 \quad (m\geqq 2)\ . \end{aligned}\right\} \tag{17}$$

Substituting (17) into (16) and after some calculations, we have:

$$\left.\begin{aligned} &I(J_0, q)\begin{cases} =kd & (q=0)\ , \\ =0 & (q\geqq 1)\ , \end{cases} \\ &I(J_{2n}, q) = 0 \qquad (n\geqq 1;\ q=0, 1, 2, \cdots)\ , \\ &I\left(\frac{J_1}{r}, q\right)\begin{cases} =\frac{1}{2}kd & (q=0)\ , \\ =0 & (q\geqq 1)\ , \end{cases} \\ &I\left(\frac{J_{2n+1}}{r}, q\right) = 0 \qquad (n\geqq 1;\ q=0, 1, 2, \cdots)\ . \end{aligned}\right\} \tag{18}$$

By use of (17), the derivatives of the Bessel functions are given as follows:

$$\left.\begin{aligned} &J_0'(z)\simeq 0, \\ &J_1'(z)\simeq\frac{1}{2}\ , \\ &J_m'(z)\simeq 0 \quad (m\geqq 2)\ . \end{aligned}\right\} \tag{19}$$

Applying the approximations (17)—(19) to the left-hand sides only of (12)—(15) (the approximation is given merely to the expressions of the buffer domain D_2), we have the following:—

$$\left.\begin{aligned} &kd\cdot\overline{\zeta}_2^{(0)} - kd\cdot\zeta_1^{(0)} = 0\ , \\ &-\frac{kd}{2}\cdot\zeta_1^{(m)} = 0 \\ &(m=1, 2, 3, \cdots)\ , \end{aligned}\right\} \tag{12'}$$

$$\left.\begin{aligned} &\frac{1}{2}kd\cdot\zeta_2^{(1)}+i\cdot kd\cdot\zeta_1^{(0)}=0\ ,\\ &i\cdot\frac{1}{2}k_1^{(m)}d\cdot\zeta_1^{(m)}=0\\ &(m=1,\ 2,\ 3,\ \cdots) \end{aligned}\right\} \tag{13'}$$

$$\left.\begin{aligned} &\overline{\zeta_2^{(0)}}+\frac{1}{\pi}kd\cdot\zeta_2^{(1)}\\ &\quad=H_0^{(1)}(kd)\cdot\zeta_3^{(0)}+2J_0(kd)\cdot\zeta_0\\ &\frac{1}{\pi}\cdot\frac{2}{1-(2m)^2}kd\cdot\zeta_2^{(1)}\\ &\quad=H_{2m}^{(1)}(kd)\cdot\zeta_3^{(2m)}+4J_{2m}(kd)\cdot\zeta_0\\ &\qquad(m=1,\ 2,\ 3,\ \cdots)\ , \end{aligned}\right\} \tag{14'}$$

$$\left.\begin{aligned} &\frac{1}{\pi}\cdot\zeta_2^{(1)}\\ &\quad=H_0^{(1)\prime}(kd)\cdot\zeta_3^{(0)}+2J_0'(kd)\cdot\zeta_0\\ &\frac{1}{\pi}\cdot\frac{2}{1-(2m)^2}\cdot\zeta_2^{(1)}\\ &\quad=H_{2m}^{(1)\prime}(kd)\cdot\zeta_3^{(2m)}+4J_{2m}'(kd)\cdot\zeta_0\\ &\qquad(m=1,\ 2,\ 3,\ \cdots)\ . \end{aligned}\right\} \tag{15'}$$

From (12′) and (13′) we have

$$\left.\begin{aligned} &\overline{\zeta_2^{(0)}}=\zeta_1^{(0)}\ ,\\ &\zeta_2^{(1)}=-i\cdot2\zeta_1^{(0)}\ ,\\ &\zeta_1^{(m)}=0\quad(m=1,\ 2,\ 3,\ \cdots) \end{aligned}\right\} \tag{20}$$

Substituting the first two expressions of (20) into the first expressions of (14′) and (15′), the following equations are obtained :—

$$\left(1-i\cdot\frac{2}{\pi}kd\right)\cdot\zeta_1^{(0)}-H_0^{(1)}(kd)\cdot\zeta_3^{(0)}=2J_0(kd)\cdot\zeta_0\ ,$$

$$-i\cdot\frac{2}{\pi}\cdot\zeta_1^{(0)}-H_0^{(1)\prime}(kd)\cdot\zeta_3^{(0)}=2J_0'(kd)\cdot\zeta_0\ .$$

Solving the above two equations, $\zeta_1^{(0)}$ and $\zeta_3^{(0)}$ are expressed as

$$\left.\begin{aligned}\zeta_1^{(0)}&=i\cdot\frac{4\zeta_0}{\Delta_0}\ ,\\ \zeta_3^{(0)}&=\frac{2\zeta_0}{\Delta_1}\left\{\left(-1+i\cdot\frac{2}{\pi}kd\right)J_1(kd)\right.\\ &\qquad\left.+i\cdot\frac{2}{\pi}J_0(kd)\right\}\ ,\end{aligned}\right\}\tag{21}$$

where

$$\left.\begin{aligned}\Delta_1&=\left(1-i\cdot\frac{2}{\pi}kd\right)H_1^{(1)}(kd)-i\cdot\frac{2}{\pi}H_0^{(1)}(kd)\ ,\\ \Delta_0&=-\pi kd\Delta_1\ .\end{aligned}\right\}\tag{21'}$$

Putting (21) into the first two equations of (20), the expressions of $\bar{\zeta}_2^{(0)}$ and $\zeta_2^{(1)}$ are :—

$$\left.\begin{aligned}\bar{\zeta}_2^{(0)}&=i\cdot\frac{4\zeta_0}{\Delta_0}\ ,\\ \zeta_2^{(1)}&=\frac{8\zeta_0}{\Delta_0}\ .\end{aligned}\right\}\tag{22}$$

By use of the expressions of (14'), (21') and (22), the higher mode of the reflected waves in the domain D_3 is expressed as

$$\zeta_3^{(2m)}=\frac{4\zeta_0}{H_{2m}^{(1)}(kd)}\cdot\left\{\frac{4}{\pi^2}\cdot\frac{1}{\Delta_1}\cdot\frac{1}{(2m)^2-1}-J_{2m}(kd)\right\}.$$

Using (17), the above equation is reduced to

$$\zeta_3^{(2m)}=\left(\frac{4}{\pi}\right)^2\cdot\frac{1}{(2m)^2-1}\cdot\frac{1}{\Delta_1}\cdot\frac{1}{H_{2m}^{(1)}(kd)}\cdot\zeta_0\tag{23}$$

$$(m=1,\ 2,\ 3,\ \cdots)\ .$$

Substituting (23) into (7), the wave height in the domain D_3 become :

$$\zeta_3=\zeta_p+\zeta_{re}^{(d)}\ ,\tag{24}$$

where

$$\left.\begin{aligned}
&\zeta_p=2\zeta_0\sum_{n=0}^{\infty}\varepsilon_n\cos 2n\theta\cdot J_{2n}(kr)\ ,\\
&\zeta_{re}^{(d)}=\zeta_3^{(0)}\cdot H_0^{(1)}(kr)+\zeta_3^{(n>0)}\ ,\\
&\zeta_3^{(n>0)}=\left(\frac{4}{\pi}\right)^2\cdot\frac{\zeta_0}{\Delta_1}\cdot\sum_{n=1}^{\infty}\frac{1}{(2n)^2-1}\cdot\frac{H_{2n}^{(1)}(kr)}{H_{2n}^{(1)}(kd)}\cdot\cos 2n\theta\ .
\end{aligned}\right\}\tag{25}$$

Likewise, the expressions of the wave heights in the domains D_1 and D_2 become as follows:

in the domain D_1,

$$\zeta_1=i\cdot\frac{4\zeta_0}{\Delta_0}\cdot e^{-iky}\ ,\tag{26}$$

which is derived from the last expression of (20), the first expression of (21) and (9);

in the domain D_2,

$$\zeta_2=\frac{4\zeta_0}{\Delta_0}\cdot\{i\cdot J_0(kr)+2\sin\theta\cdot J_1(kr)\}\ .\tag{27}$$

In the last expression, the equations (8) and (22) are used, and the terms beyond $\overline{\zeta_2^{(0)}}$ and $\zeta_2^{(1)}$ are neglected, because no contribution of these terms upon ζ_2 may be considered under the approximation (17) used in this section.

Before proceeding to the numerical calculation and discussion, the applicability of the theory derived under the first approximation is discussed in the following.

From the expression of the ascending series of the Bessel function

$$\left.\begin{aligned}
&J_m(z)=\left(\frac{z}{2}\right)^m\sum_{n=0}^{\infty}\frac{(-1)^n}{n!(m+n)!}\left(\frac{z}{2}\right)^{2n}\\
&\qquad(m=0,\ 1,\ 2,\ \cdots)
\end{aligned}\right\}\tag{28}$$

and the approximated ones of (17), the errors due to the first approximation (17) are estimated as follows[4]:—

4) The Bessel function (28) is an alternating convergent series with a maximum absolute value at a certain term which is relevant to the magnitude of the variable z. Therefore, in order to estimate the errors of the approximation, we must prescribe the range of the argument z allowing for the convergence of the series. When the series is an alternating one, if the n-th term is in magnitude smaller than the $(n-1)$-th one for a sufficiently large n, such a series is called to be convergent. Hence the determination of the range of the argument z so as to make possible the estimation of the errors must

an error from the approximation $J_0(z)\simeq 1$ is about

$$\left(\frac{z}{2}\right)^2 \text{ for the values in the range } |z|<4\,; \tag{29}$$

an error from the approximation $J_1(z)\simeq\frac{z}{2}$ about

$$\frac{1}{2!}\left(\frac{z}{2}\right)^3 \text{ for } |z|<2\sqrt{6}\,; \tag{30}$$

an error from the approximation $J_m(z)\simeq 0$ $(m=2, 3, 4, \cdots)$ about

$$\frac{1}{m!}\left(\frac{z}{2}\right)^m \text{ for } |z|<2\sqrt{m+1}\,. \tag{31}$$

From (29)—(31), the error of the present appoximation is considered to be approximately

$$\left(\frac{z}{2}\right)^2 \text{ for } |z|<2\sqrt{3}\,. \tag{32}$$

Although the above estimation of the error has been made in the absolute value, the error (32) is interpreted as a relative one because the first term of $J_0(z)$ is a unit.

Now, by use of (26) and (21′), the variation of the wave height in the domain D_1 versus kd is examined numerically. Taking account of the application range (32) of the theory, the parameter kd is varied from 0 to 2. Then the expected error (a relative one) is $\left(\frac{kd}{2}\right)^2$ on the highest estimate. The calculated values of the wave height, $\arg\zeta_1^{(0)}$ and

---

be carried out in such a way that

|the n-th term| > |the $(n+1)$-th term| for $n\geqq n_0$, where |the n_0-th term| is supposed to be the error of the finite series up to the (n_0-1)-th term.

Hence if we retain the terms up to (n_0-1) in the series of the Bessel function $J_m(z)$, the error due to the truncation of the series is

$$\frac{1}{n_0!\cdot(m+n_0)!}\left(\frac{z}{2}\right)^{m+2n_0} \qquad (at\ most) \qquad (\mathrm{I})$$

and the range of z to make possible the above estimation of the error is derived from an inequality

$$\frac{1}{n_0!\cdot(m+n_0)!}\left(\frac{z}{2}\right)^{m+2n_0} > \frac{1}{(n_0+1)!\cdot(m+n_0+1)!}\left(\frac{z}{2}\right)^{m+2n_0+2},$$

i. e.

$$|z|<2\sqrt{(n_0+1)(m+n_0+1)} \qquad (\mathrm{II})$$

Using (I) and (II), the estimations of the errors in (29) to (31) are made.

β are tabulated in Table 1, of which the graphs are drawn in Figs. 2, 3 and 4 respectively. Here, β is defined as follows.

Setting down

$$\beta=(\arg \zeta_1^{(0)})/kd\ , \tag{33}$$

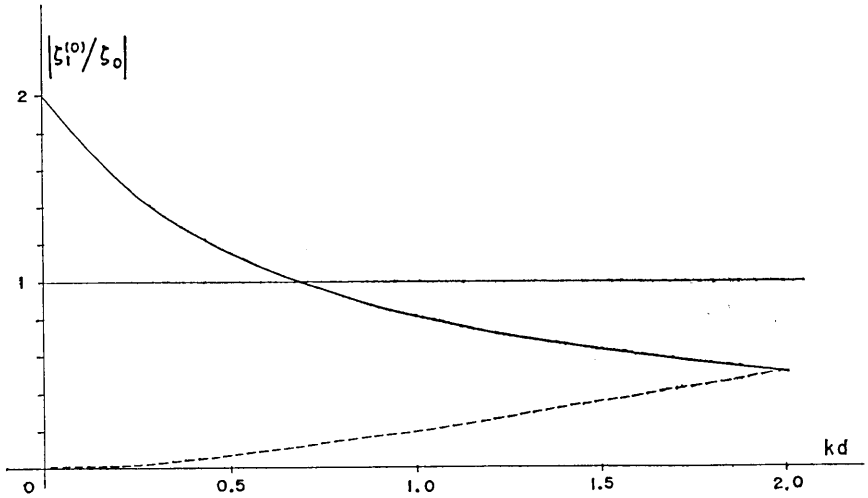

Fig. 2. The variation of the wave height in the canal (the full line is the variation of the wave height calculated based on the theory of the first approximation and the broken line the estimated errors).

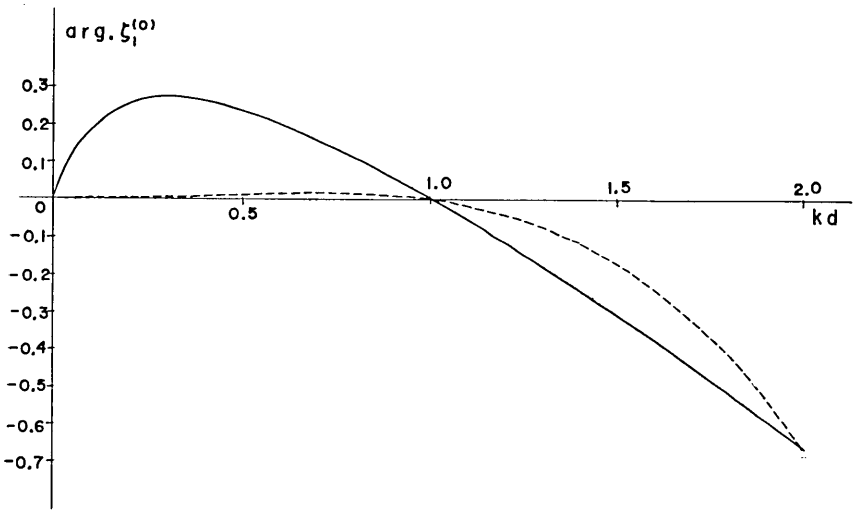

Fig. 3. The variation of $\arg \zeta_1^{(0)}$ versus kd (the solid line is the variation of $\arg \zeta_1^{(0)}$ for a change of kd and the broken line the estimated errors).

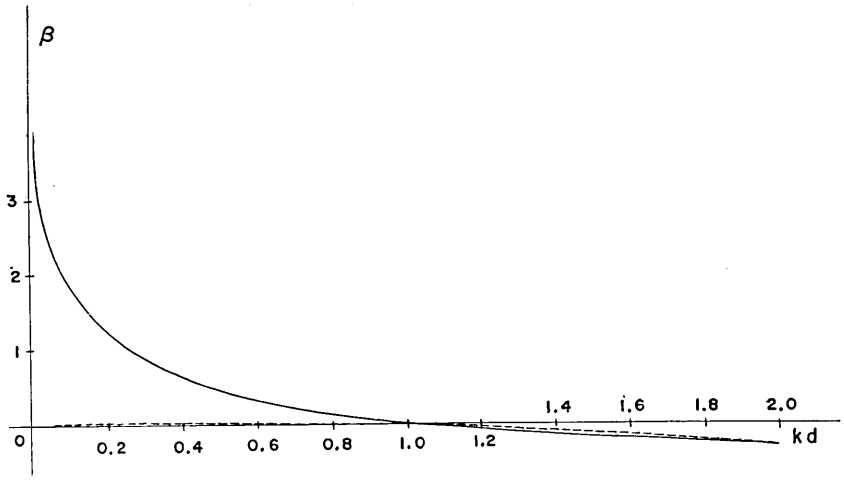

Fig. 4. The variation of β-value versus kd (the full line stands for the variation of the computed values of β and the broken line the estimated errors).

the expression (26) is transformed into

$$\zeta_1=|\zeta_1|\exp\{-ik^*(y^*-\beta)\}\ , \tag{34}$$

where

$$\left.\begin{aligned} k^*&=kd\ ,\\ y^*&=y/d\ ,\end{aligned}\right\}\ \text{(in dimensionless form with respect to } d)\ ,$$

and where, since no higher modes of the waves exist in the expression (26), the following identity holds, i. e.

$$|\zeta_1|\equiv|\zeta_1^{(0)}|\ .$$

Allowing for the omitted time factor $\exp(-i\omega t)$ and taking the real part, the complete form of the waves in the domain D_1 is

$$\zeta_1=|\zeta_1^{(0)}|\cos\{\omega t+k^*(y^*-\beta)\}\ , \tag{35}$$

or

$$\zeta_1=|\zeta_1^{(0)}|\cos(\omega t+k^*y^*-\arg\zeta_1^{(0)})\ . \tag{36}$$

In the above two expressions, the former is preferred to inspect at what position of the y-coordinate a wave of the type $\cos(\omega t+ky)$ is originated, and the latter to see at what extent the progressive wave in the domain D_1 has a phase difference at the mouth of the canal ($y=0$).

Table 1. The variations of the waves in the domain D_1 versus kd.

kd	$\lvert\zeta_1^{(0)}\rvert/\zeta_0$	$\arg\zeta_1^{(0)}$	β
0.02	1.95523	0.062323	3.11616
0.04	1.90697	0.104274	2.60681
0.06	1.85811	0.137341	2.28903
0.08	1.80989	0.164225	2.05282
0.10	1.76295	0.186336	1.86336
0.12	1.71767	0.204581	1.70484
0.14	1.67420	0.219608	1.56862
0.16	1.63262	0.231906	1.44941
0.18	1.59292	0.241860	1.34366
0.20	1.55507	0.249780	1.24890
0.22	1.51900	0.255921	1.16327
0.24	1.48463	0.260495	1.08539
0.26	1.45187	0.263681	1.01415
0.28	1.42063	0.265630	0.94867
0.30	1.39083	0.266473	0.88824
0.32	1.36236	0.266323	0.83225
0.34	1.33516	0.265275	0.78022
0.36	1.30915	0.263416	0.73171
0.38	1.28424	0.260819	0.68636
0.40	1.26038	0.257550	0.64387
0.42	1.23749	0.253666	0.60396
0.44	1.21552	0.249218	0.56640
0.46	1.19440	0.244253	0.53098
0.48	1.17410	0.238809	0.49751
0.50	1.15455	0.232924	0.46584
0.52	1.13571	0.226630	0.43582
0.54	1.11755	0.219956	0.40732
0.56	1.10002	0.212928	0.38022
0.58	1.08309	0.205571	0.35443
0.60	1.06672	0.197906	0.32984
0.62	1.05088	0.189952	0.30637
0.64	1.03555	0.181727	0.28394
0.66	1.02069	0.173247	0.26249
0.68	1.00629	0.164527	0.24195
0.70	0.99231	0.155581	0.22226
0.72	0.97875	0.146421	0.20336
0.74	0.96557	0.137058	0.18521
0.76	0.95275	0.127503	0.16776
0.78	0.94029	0.117766	0.15098
0.80	0.92816	0.107854	0.13481
0.82	0.91635	0.097777	0.11924
0.84	0.90485	0.087542	0.10421
0.86	0.89363	0.077156	0.08971
0.88	0.88269	0.066625	0.07571
0.90	0.87201	0.055955	0.06217
0.92	0.86159	0.045153	0.04907
0.94	0.85141	0.034222	0.03640
0.96	0.84147	0.023168	0.02413
0.98	0.83174	0.011996	0.01224
1.00	0.82224	0.000709	0.00070

(to be continued)

(continued)

kd	$\lvert\zeta_1^{(0)}\rvert/\zeta_0$	$\arg\zeta_1^{(0)}$	β
1.02	0.81294	−0.010687	−0.01047
1.04	0.80383	−0.022191	−0.02133
1.06	0.79492	−0.033798	−0.03188
1.08	0.78619	−0.045506	−0.04213
1.10	0.77764	−0.057311	−0.05210
1.12	0.76926	−0.069210	−0.06179
1.14	0.76104	−0.081200	−0.07122
1.16	0.75299	−0.093280	−0.08041
1.18	0.74508	−0.105447	−0.08936
1.20	0.73733	−0.117698	−0.09808
1.22	0.72972	−0.130031	−0.10658
1.24	0.72224	−0.142445	−0.11487
1.26	0.71490	−0.154937	−0.12296
1.28	0.70770	−0.167507	−0.13086
1.30	0.70061	−0.180151	−0.13857
1.32	0.69365	−0.192869	−0.14611
1.34	0.68681	−0.205658	−0.15347
1.36	0.68008	−0.218519	−0.16067
1.38	0.67347	−0.231448	−0.16771
1.40	0.66696	−0.244445	−0.17460
1.42	0.66056	−0.257509	−0.18134
1.44	0.65426	−0.270638	−0.18794
1.46	0.64806	−0.283831	−0.19440
1.48	0.64196	−0.297087	−0.20073
1.50	0.63595	−0.310405	−0.20693
1.52	0.63004	−0.323785	−0.21301
1.54	0.62421	−0.337224	−0.21897
1.56	0.61847	−0.350723	−0.22482
1.58	0.61282	−0.364279	−0.23055
1.60	0.60725	−0.377894	−0.23618
1.62	0.60176	−0.391564	−0.24170
1.64	0.59635	−0.405291	−0.24712
1.66	0.59102	−0.419072	−0.25245
1.68	0.58576	−0.432908	−0.25768
1.70	0.58058	−0.446797	−0.26282
1.72	0.57547	−0.460739	−0.26787
1.74	0.57043	−0.474733	−0.27283
1.76	0.56546	−0.488779	−0.27771
1.78	0.56056	−0.502875	−0.28251
1.80	0.55572	−0.517022	−0.28723
1.82	0.55095	−0.531218	−0.29187
1.84	0.54624	−0.545463	−0.29644
1.86	0.54160	−0.559757	−0.30094
1.88	0.53701	−0.574098	−0.30537
1.90	0.53249	−0.588487	−0.30972
1.92	0.52802	−0.602922	−0.31402
1.94	0.52361	−0.617404	−0.31824
1.96	0.51926	−0.631932	−0.32241
1.98	0.51496	−0.646505	−0.32651
2.00	0.51072	−0.661123	−0.33056

As shown in Fig. 2, the amplitude of ζ_1 tends to double that of the invading waves in the open sea, when $kd \to 0$. Starting from $kd=0$, $|\zeta_1|$ decreases rapidly to the value[5] of about 1.0 as kd increasing to 0.7, and then the rate of decrease of $|\zeta_1|$ becomes gradually small when the argument kd further increases. It is noteworthy that, when kd increases beyond about 0.7, the wave height in the domain D_1 becomes smaller than 1.0 in magnitude. It is thought that, from past experience, $|\zeta_1|$ approaches a unit when kd increases. For the result computed above, one of the possible explanations is attributed to the fact that the present theory developed in the first approximation cannot be applied to the range beyond $kd=$about 0.7. In order to examine this possibility, the probable error estimated from (32) is inserted in Fig. 2, which is shown by the broken line (in the absolute errors).[6] An shown in Fig. 2, the absolute error for $kd=1.0$ is about 0.2 at most. Suppose that all of the error 0.2 contributes to the wave height $|\zeta_1|$, the value of $|\zeta_1|$ is 1.0222 which is considered to be plausible in magnitude from our experience, according to which $|\zeta_1|$ seems to have to exceed 1.0. Likewise, the absolute error for $kd=2.0$ is about 0.5. Then if 0.5 should be added to the value of $|\zeta_1|$, the corrected $|\zeta_1|$ is nearly equal to a unit. Hence the paradox that the curve of $|\zeta_1|$ values transverses the line of $|\zeta_1|=1.0$ is explained by the correction of the error.

At any rate, from the above examination, we may come to the conclusion that, when $kd=1.0$, the height of the waves propagated in the domain D_1 does not completely become affected by the shape of an estuary.

Next, let us consider the behavior of the phase. In Figs. 3 and 4, the inserted broken lines stand for the absolute errors calculated from (32). In both figures, the most conspicuous features are those that, when kd approaches a unit, $\arg \zeta_1^{(0)}$ and β take zero values.

As far as the variation of $\arg \zeta_1^{(0)}$ is concerned, it has a maixmum value at the point $kd=$about 0.3. On the lower side of this point, $\arg \zeta_1^{(0)}$ value diminishes to zero, while, on the upper side, the value decreases monotonically crossing the zero line. As shown in Fig. 3, the absolute error amounts to not a little magnitude in the range above $kd=1.5$, so that the theory of the present approximation is considered

---

5) The value of the wave height ζ_1 has a unit ζ_0. Therefore, the value 1.0 stands for $1.0\times\zeta_0$ and this convention is followed in the following discussion.

6) The values of the *probable* absolute errors computed from (32) are tabulated in Table 2.

Table 2. The absolute errors of $|\zeta_1|/\zeta_0$, $\arg\zeta_1^{(0)}$ and β estimated approximately.

kd	$\lvert\zeta_1\rvert/\zeta_0$	$\arg\zeta_1^{(0)}$	β
0.1	0.00441	0.00046	0.00465
0.2	0.01555	0.00249	0.01248
0.3	0.03129	0.00599	0.01998
0.4	0.05041	0.01030	0.02575
0.5	0.07216	0.01455	0.02911
0.6	0.09600	0.01781	0.02968
0.7	0.12155	0.01905	0.02722
0.8	0.14851	0.01725	0.02156
0.9	0.17658	0.01133	0.01259
1.0	0.20556	0.00017	0.00017
1.1	0.23524	−0.01733	−0.01576
1.2	0.26544	−0.04236	−0.03531
1.3	0.29601	−0.07611	−0.05855
1.4	0.32681	−0.11977	−0.08555
1.5	0.35772	−0.17460	−0.11640
1.6	0.38864	−0.24185	−0.15115
1.7	0.41947	−0.32281	−0.18988
1.8	0.45012	−0.41878	−0.23366
1.9	0.48049	−0.53110	−0.27953
2.0	0.51072	−0.66112	−0.33056

to be in use supposedly in the range $kd=0$ to at most 1.5. At any rate, the result obtained in Fig. 3 is physically acceptable such that, when a length of the incident waves (λ) is large as compared with a width of the canal (d), little effect of the form of an estuary appears on the phase of the progressive waves in the domain D_1. And when λ decreasing in magnitude for d, the phase increases to a certain maximum value and later decreases monotonically until the value of the phase becomes a negative one. The last phenomenon is interpreted to be due to the fact that, when d becomes large for λ, the corner of the mouth of the canal does not effect its influence very easily upon the waves in the central part of the canal. When kd tends to zero, $\arg\zeta_1^{(0)}$ approaches zero value, but β increases to an infinitely large value, as seen in Fig. 4. From the expression (35), the β value is interpreted as a position at which $\cos(\omega t+ky)$-type waves are supposedly originated on the y-coordinate. Allowing for the above mentioned fact and from Fig. 4, it turns out that the $\cos(\omega t+ky)$-type waves propagated into the canal have

a hypothetical origin at an infinite point in the open sea, when kd limits to zero.

Now, a consideration of the waves in the domain D_2 is made in the following.

Using the first equation of (21), the expression (27) becomes

$$\zeta_2=\zeta_1^{(0)}\{J_0(k^*r^*)-i\cdot 2J_1(k^*r^*)\sin\theta\} \tag{37}$$

in a form excepting the time factor, where $r^*=r/d$.

Then

$$\left.\begin{aligned}|\zeta_2|&=|\zeta_1^{(0)}|\sqrt{J_0^2(k^*r^*)+4J_1^2(k^*r^*)\sin^2\theta}\,,\\ \arg\zeta_2&=\arg\zeta_1^{(0)}-\tan^{-1}\left\{\frac{J_1(k^*r^*)}{J_0(k^*r^*)}\sin\theta\right\}.\end{aligned}\right\} \tag{38}$$

If the time factor is included, the above expression is re-arranged in the form

$$\zeta_2=|\zeta_2|\cos(\omega t-\arg\zeta_2)\,, \tag{39}$$

where the only real part is retained.

When $\theta=0$ or π, (39) is reduced to

$$\zeta_2=|\zeta_1^{(0)}|\cos(\omega t-\arg\zeta_1^{(0)})\,,$$

which is equal to the wave height in the domain D_1 at $y=0$ (refer to (36)).

When the radial component r is increased (then the azimuthal component θ is fixed), the amplitude factor $|\zeta_2|$ is augmented monotonically, the variation of which is most conspicuous in the direction perpendicular to the coast.

Since, in the domain D_2, the variable r is smaller than d, the approximation (17) can be applied to the Bessel functions in (37) and (38). Then the expression of the wave height in the domain D_2 is obtained in a further simplified form:

from (37),

$$\zeta_2=\zeta_1^{(0)}(1-i\cdot k^*r^*\sin\theta) \tag{37'}$$

from (38),

$$\left.\begin{aligned}|\zeta_2|&=|\zeta_1^{(0)}|\sqrt{1+(k^*r^*\sin\theta)^2}\\ \arg\zeta_2&=\arg\zeta_1^{(0)}-\tan^{-1}(k^*r^*\sin\theta)\end{aligned}\right\} \tag{38'}$$

Although the above expressions have accessible forms to the discussion of the behavior of the waves in the domain D_1, there exists some disadvantage with respect to the continuity between the neighbouring domains. In the domain D_3, the approximation (17) cannot be applied because the argument r goes beyond the application range of (17), so that the reduction by use of (17) cannot be made. Hence the continuity of the waves between the adjacent domains D_2 and D_3 do not hold owing to the partial assessment of the approximation and the amount of the discontinuity is of the order of the error estimated from (32).

Introducing the Cartesian co-ordinates, (37′) and (38′) are reduced further to the following forms :—

$$\left.\begin{aligned} &\zeta_2=\zeta_1^{(0)}(1-i\cdot k^*y^*)\ , \\ &|\zeta_2|=|\zeta_1^{(0)}|\sqrt{1+(k^*y^*)^2}\ , \\ &\arg\zeta_2=\arg\zeta_1^{(0)}-\tan^{-1}(k^*y^*)\ , \end{aligned}\right\} \tag{40}$$

where $y^*=y/d$.

From the expression (40), it is found that the equi-amplitude and equi-phase lines run parallel to the straight coast.

Supposing that the approximations for sine and cosine functions,

$$\left.\begin{aligned} &\sin(k^*y^*)\simeq k^*y^* \\ &\cos(k^*y^*)\simeq 1 \end{aligned}\right\}\ ,$$

are possible, of which the convergence is not so good as that of the ascending series of the Bessel function (28), the equation (40) is likely to be transformed into

$$\left.\begin{aligned} &\zeta_2=\zeta_1^{(0)}\exp(-i\cdot k^*y^*)\ , \\ &|\zeta_2|=|\zeta_1^{(0)}|\ ,\ \arg\zeta_2=\arg\zeta_1^{(0)}-k^*y^*\ . \end{aligned}\right\}$$

When the time factor is involved, the above equations become as follows :—

$$\zeta_2=|\zeta_1^{(0)}|\cos(\omega t+k^*y^*-\arg\zeta_1^{(0)})\ , \tag{41}$$

where the only real part is retained.

From the above expression, we find that the waves in front of the mouth of the canal leading to the open sea are propagated into the canal with a period and wave length of the incident waves.

Next, we proceed to the discussion of the behavior of the waves in the domain D_3. As far as the waves in the domain D_3 are concerned, our greatest interest is for the directivity and a rate of decay of the diverging waves, which are investigated from (24) and (25). The second term of (24), i.e., $\zeta_{re}^{(d)}$ denotes the damping reflected waves, instead of merely reflected ones, in the open sea. By use of this expression and an electronic computer, the behaviors of the damping reflected waves are inquired into in the following.

The variations of the amplitudes of $\zeta_{re}^{(d)}$ for a change of the radial component r^* $(=r/d)$ are shown figuratively in Figs. 5 (then k^* $(=kd)$ and the azimuthal component θ are parameters), of which the values are tabulated in Tables 3.

From Figs 5, it turns out that :[7]—

When k^* is very small, little contribution of the damping reflected waves to the standing waves, ζ_p in (24), is made, of which the order is, for $k^*=0.02$, about 10 percent of the amplitude of the incident waves in the nearby part of an estuary and becomes less than 10 percent when departing from the mouth of the canal.

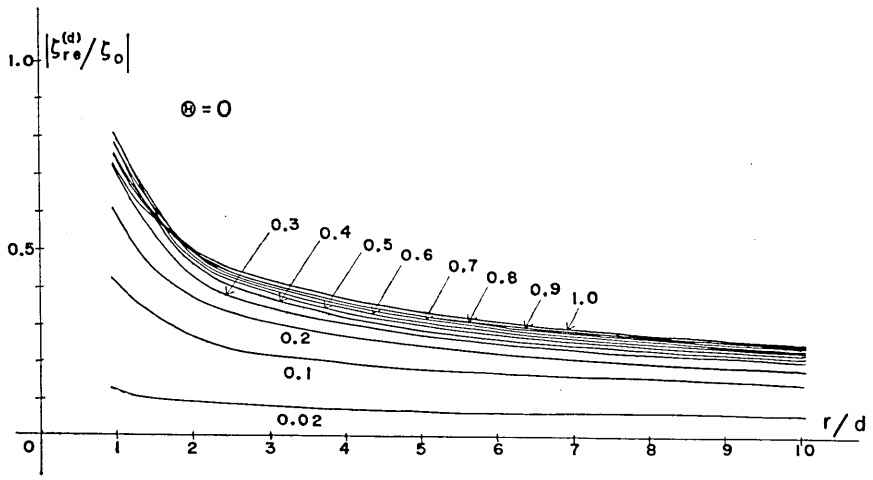

Fig. 5a. The variation of the heights of the damping reflected waves in the direction of $\theta=0$ for a change of r/d (the curves with the stated values stand for those relevant to the relative wave numbers $kd=0.02, 0.1, \cdots, 1.0$).

7) In Figs. 5, the curves for stated parameters $k^*=0.7\sim1.0$ intersect at the nearby part of $r^*=1.0$, but these intersections are considered to be due to the approximation employed in the derivation of the theory. When k^* becomes large, little validity for the theory of the first approximation exists.

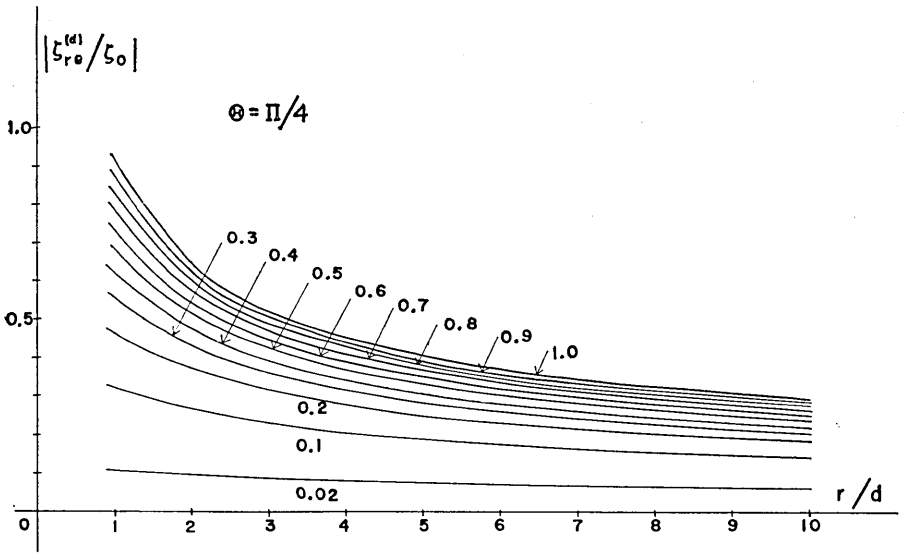

Fig. 5b. The variation of the heights of the damping reflected waves in the direction of $\theta=\pi/4$ for a change of r/d (the curves with the stated values stand for those relevant to the relative wave numbers $kd=0.02, 0.1, \cdots, 1.0$).

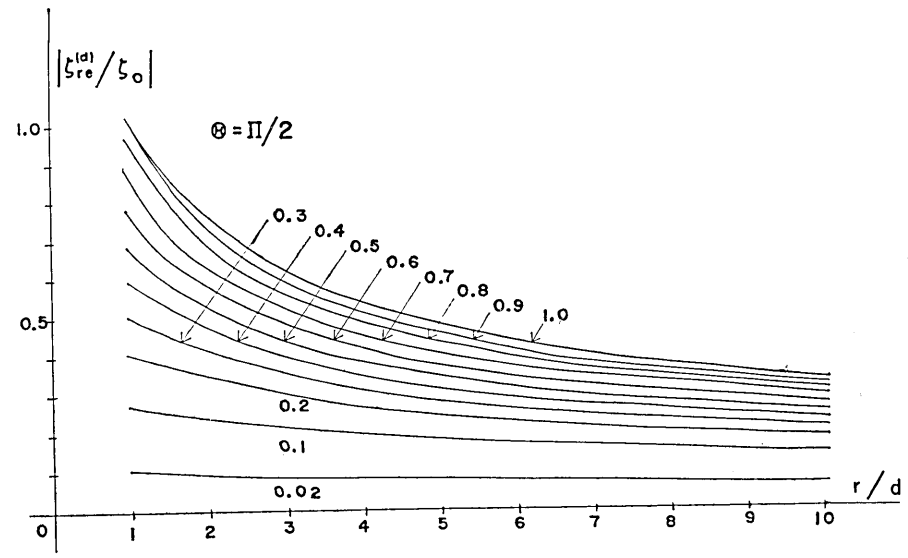

Fig. 5c. The variation of the heights of the damping reflected waves in the direction of $\theta=\pi/2$ for a change of r/d (the curves with the stated values stand for those relevant to the relative wave numbers $kd=0.02, 0.1, \cdots, 1.0$).

When k^* increases, a contribution of the damping reflected waves to the standing waves is also augmented. Along the coast ($\theta=0$), the value of $\zeta_{re}^{(d)}$ for $k^*=1.0$ amounts to 70 percent of the height of the incident waves at a point $r^*=1.0$ and about 25 percent at $r^*=10.0$. As azimuthal component θ increases (a line tracing the variation of the wave height is directed in a sense perpendicular to the coast facing the open sea), the heights of the damping reflected waves are upheaved. In the direction leading to the canal, these magnitudes are most conspicuous such that the contribution of $\zeta_{re}^{(d)}$ amounts to almost one hundred percent of the amplitude of the surging waves at $r^*=1.0$ and about 45 percent $r^*=10.0$.

As far as the variations of the heights of the damping reflected waves versus a parameter k^* is concerned, another outstanding feature is found such that the curves showing the variations of the wave heights seem to tend to certain asymptotic curves as k^* increases. In other words, when a wave length of the incident waves becomes large as compared with a width of the canal, the surface made by the *damping* reflected waves (instead of reflected waves) is likely to tend to a certain asymptotic surface.

As far as the damping rate of $|\zeta_{re}^{(d)}|$ is concerned, when a wave length of the incident waves is long as compared with a width of the canal, the rate of the damping is very gentle, while, as k^* increases, the damping rate of $|\zeta_{re}^{(d)}|$ also increases, especially in the nearby part of the mouth of the canal. The damping rate considered here is that against a dimensionless value r^* $(=r/d)$, but it might be preferred to discuss a rate of damping for a variation of positions r/λ, which is made dimensionless with respect to a wave length of the incident waves instead of a width of the canal. The last treatment will be made in future.

In the next paper, a theory will be developed up to the second approximation.

Table 3a. The wave heights of the damping

r^* \ k^*	0.02	0.1	0.2	0.3	0.4
1.0	0.12842×10^{0}	0.41009×10^{0}	0.59752×10^{0}	0.70186×10^{0}	0.75853×10^{0}
2.0	0.96015×10^{-1}	0.27385×10^{0}	0.37676×10^{0}	0.42964×10^{0}	0.45903×10^{0}
3.0	0.84422×10^{-1}	0.22986×10^{0}	0.30941×10^{0}	0.34959×10^{0}	0.37247×10^{0}
4.0	0.77419×10^{-1}	0.20367×10^{0}	0.27038×10^{0}	0.30386×10^{0}	0.32324×10^{0}
5.0	0.72352×10^{-1}	0.18527×10^{0}	0.24356×10^{0}	0.27275×10^{0}	0.28986×10^{0}
6.0	0.68399×10^{-1}	0.17128×10^{0}	0.22352×10^{0}	0.24967×10^{0}	0.26518×10^{0}
7.0	0.65178×10^{-1}	0.16011×10^{0}	0.20776×10^{0}	0.23165×10^{0}	0.24593×10^{0}
8.0	0.62476×10^{-1}	0.15089×10^{0}	0.19492×10^{0}	0.21705×10^{0}	0.23036×10^{0}
9.0	0.60163×10^{-1}	0.14312×10^{0}	0.18420×10^{0}	0.20489×10^{0}	0.21743×10^{0}
10.0	0.58151×10^{-1}	0.13643×10^{0}	0.17507×10^{0}	0.19458×10^{0}	0.20645×10^{0}

Table 3b. The wave heights of the damping

r^* \ k^*	0.02	0.1	0.2	0.3	0.4
1.0	0.10930×10^{0}	0.31544×10^{0}	0.45197×10^{0}	0.54147×10^{0}	0.61130×10^{0}
2.0	0.91559×10^{-1}	0.25924×10^{0}	0.36029×10^{0}	0.42091×10^{0}	0.46521×10^{0}
3.0	0.82637×10^{-1}	0.22465×10^{0}	0.30595×10^{0}	0.35334×10^{0}	0.38753×10^{0}
4.0	0.76361×10^{-1}	0.20129×10^{0}	0.27040×10^{0}	0.31013×10^{0}	0.33873×10^{0}
5.0	0.71573×10^{-1}	0.18407×10^{0}	0.24483×10^{0}	0.27953×10^{0}	0.30453×10^{0}
6.0	0.67726×10^{-1}	0.17067×10^{0}	0.22530×10^{0}	0.25641×10^{0}	0.27886×10^{0}
7.0	0.64527×10^{-1}	0.15982×10^{0}	0.20975×10^{0}	0.23815×10^{0}	0.25871×10^{0}
8.0	0.61798×10^{-1}	0.15081×10^{0}	0.19700×10^{0}	0.22328×10^{0}	0.24234×10^{0}
9.0	0.59427×10^{-1}	0.14315×10^{0}	0.18629×10^{0}	0.21085×10^{0}	0.22871×10^{0}
10.0	0.57337×10^{-1}	0.13655×10^{0}	0.17714×10^{0}	0.20028×10^{0}	0.21714×10^{0}

Table 3c. The wave heights of the damping

r^* \ k^*	0.02	0.1	0.2	0.3	0.4
1.0	0.94196×10^{-1}	0.27572×10^{0}	0.40546×10^{0}	0.50317×10^{0}	0.59751×10^{0}
2.0	0.87940×10^{-1}	0.24793×10^{0}	0.34919×10^{0}	0.41845×10^{0}	0.47720×10^{0}
3.0	0.81099×10^{-1}	0.22008×10^{0}	0.30353×10^{0}	0.35821×10^{0}	0.40340×10^{0}
4.0	0.75500×10^{-1}	0.19911×10^{0}	0.27075×10^{0}	0.31673×10^{0}	0.35437×10^{0}
5.0	0.71031×10^{-1}	0.18296×10^{0}	0.24624×10^{0}	0.28643×10^{0}	0.31921×10^{0}
6.0	0.67357×10^{-1}	0.17011×10^{0}	0.22715×10^{0}	0.26319×10^{0}	0.29254×10^{0}
7.0	0.64262×10^{-1}	0.15957×10^{0}	0.21179×10^{0}	0.24468×10^{0}	0.27147×10^{0}
8.0	0.61599×10^{-1}	0.15074×10^{0}	0.19911×10^{0}	0.22953×10^{0}	0.25432×10^{0}
9.0	0.59274×10^{-1}	0.14320×10^{0}	0.18840×10^{0}	0.21682×10^{0}	0.24000×10^{0}
10.0	0.57216×10^{-1}	0.13667×10^{0}	0.17922×10^{0}	0.20599×10^{0}	0.22784×10^{0}

8) These values were computed by the series

$$\zeta_{re}^{(d)}/\zeta_0=\sum_{n=0}^{N-1}(\zeta_3^{(2n)}/\zeta_0)\cdot\cos 2n\theta\cdot H_{2n}^{(1)}(kr)\ ,$$

where N is taken as 11. Then the omitted first term $(\zeta^{(2N)}/\zeta_0)\cdot\cos 2nN\theta\cdot H_{2N}^{(1)}(kr)$ is of

reflected waves in the direction $\theta=0$.[8)]

0.5	0.6	0.7	0.8	0.9	1.0
0.78779×10^{0}	0.79550×10^{0}	0.78851×10^{0}	0.77019×10^{0}	0.74303×10^{0}	0.70880×10^{0}
0.47576×10^{0}	0.48511×10^{0}	0.48993×10^{0}	0.49193×10^{0}	0.49224×10^{0}	0.49153×10^{0}
0.38655×10^{0}	0.39577×10^{0}	0.40222×10^{0}	0.40711×10^{0}	0.41085×10^{0}	0.41420×10^{0}
0.33566×10^{0}	0.34437×10^{0}	0.35099×10^{0}	0.35637×10^{0}	0.36110×10^{0}	0.36550×10^{0}
0.30112×10^{0}	0.30931×10^{0}	0.31578×10^{0}	0.32125×10^{0}	0.32619×10^{0}	0.33071×10^{0}
0.27556×10^{0}	0.28328×10^{0}	0.28953×10^{0}	0.29494×10^{0}	0.29985×10^{0}	0.30443×10^{0}
0.25563×10^{0}	0.26295×10^{0}	0.26895×10^{0}	0.27421×10^{0}	0.27901×10^{0}	0.28353×10^{0}
0.23949×10^{0}	0.24646×10^{0}	0.25224×10^{0}	0.25733×10^{0}	0.26201×10^{0}	0.26642×10^{0}
0.22608×10^{0}	0.23275×10^{0}	0.23831×10^{0}	0.24325×10^{0}	0.24779×10^{0}	0.25207×10^{0}
0.21471×10^{0}	0.22110×10^{0}	0.22647×10^{0}	0.23125×10^{0}	0.23567×10^{0}	0.23981×10^{0}

reflected waves in the direction $\theta=\pi/4$.[8)]

0.5	0.6	0.7	0.8	0.9	1.0
0.67221×10^{0}	0.72761×10^{0}	0.77953×10^{0}	0.82822×10^{0}	0.87340×10^{0}	0.91457×10^{0}
0.50206×10^{0}	0.53498×10^{0}	0.56531×10^{0}	0.59341×10^{0}	0.61920×10^{0}	0.64240×10^{0}
0.41586×10^{0}	0.44119×10^{0}	0.46458×10^{0}	0.48629×10^{0}	0.50622×10^{0}	0.52415×10^{0}
0.36249×10^{0}	0.38381×10^{0}	0.40356×10^{0}	0.42194×10^{0}	0.43885×10^{0}	0.45407×10^{0}
0.32536×10^{0}	0.34413×10^{0}	0.36156×10^{0}	0.37781×10^{0}	0.39278×10^{0}	0.40628×10^{0}
0.29765×10^{0}	0.31460×10^{0}	0.33039×10^{0}	0.34513×10^{0}	0.35872×10^{0}	0.37098×10^{0}
0.27594×10^{0}	0.29154×10^{0}	0.30608×10^{0}	0.31967×10^{0}	0.33222×10^{0}	0.34354×10^{0}
0.25836×10^{0}	0.27288×10^{0}	0.28644×10^{0}	0.29912×10^{0}	0.31083×10^{0}	0.32140×10^{0}
0.24375×10^{0}	0.25739×10^{0}	0.27014×10^{0}	0.28208×10^{0}	0.29311×10^{0}	0.30306×10^{0}
0.23135×10^{0}	0.24427×10^{0}	0.25634×10^{0}	0.26765×10^{0}	0.27810×10^{0}	0.28754×10^{0}

reflected waves in the direction $\theta=\pi/2$.[8)]

0.5	0.6	0.7	0.8	0.9	1.0
0.68670×10^{0}	0.77409×10^{0}	0.86721×10^{0}	0.94942×10^{0}	$0.10139\times10^{+1}$	$0.10831\times10^{+1}$
0.53215×10^{0}	0.58524×10^{0}	0.63664×10^{0}	0.68578×10^{0}	0.73191×10^{0}	0.77433×10^{0}
0.44521×10^{0}	0.48552×10^{0}	0.52457×10^{0}	0.56205×10^{0}	0.59733×10^{0}	0.62984×10^{0}
0.38910×10^{0}	0.42259×10^{0}	0.45511×10^{0}	0.48641×10^{0}	0.51585×10^{0}	0.54305×10^{0}
0.34944×10^{0}	0.37863×10^{0}	0.40701×10^{0}	0.43428×10^{0}	0.46010×10^{0}	0.48394×10^{0}
0.31962×10^{0}	0.34581×10^{0}	0.37130×10^{0}	0.39585×10^{0}	0.41905×10^{0}	0.44057×10^{0}
0.29622×10^{0}	0.32015×10^{0}	0.34348×10^{0}	0.36592×10^{0}	0.38717×10^{0}	0.40694×10^{0}
0.27723×10^{0}	0.29941×10^{0}	0.32105×10^{0}	0.34191×10^{0}	0.36166×10^{0}	0.38000×10^{0}
0.26144×10^{0}	0.28221×10^{0}	0.30247×10^{0}	0.32202×10^{0}	0.34044×10^{0}	0.35763×10^{0}
0.24805×10^{0}	0.26764×10^{0}	0.28676×10^{0}	0.30522×10^{0}	0.32265×10^{0}	0.33882×10^{0}

---

the order of about 10^{-3}, according to numerical experiments.

20. 河口近傍における長波について [I] (buffer domain の方法による解析)

地震研究所　桃　井　高　夫

本論文においては河口附近における長波に関する研究が，buffer domain の方法を用いてなされている．まず全領域は3つの部分に分けられる．そのうち1つは buffer domain である．そして河口部と広海 (open sea) はベッセル函数を用いて解が求められ，水路の部分は三角函数を用いて解が表現されている．得られた解の数値計算には電子計算機が用いられ，次のような結論を得た．

(1) 水路に進入する波について

kd (k は広海における進入波の波数，d は水路の幅の半分の長さ) が零に近づくにつれて水路の波の波高は広海における進入波の波高の2倍に近づき，位相のずれは零に近づく，そして水路の進入波は恰も無限遠点を起点としているかのごとくである．

kd が増加するにつれて波高は単調に減少し，kd が約 1.0 のあたりではほとんど水路への進入波は開口部 (水路の広海につながる部分) の影響を受けずに水路の中へ進む．すなわち，水路の波高は広海の進入波の波高とほとんど等しい．

位相のずれに関しては kd が増加するにつれて，その値は増加し，kd がおよそ 0.3 のあたりで極値を取り，再び値は下降し kd が約 1.0 の所で零となり次いで負の値をとる．

そして水路への進入波の仮想的な原点は広海の無限遠点より河口に急速に，kd の増加につれて近づく．

(2) 水路の開口部における波について

正弦，余弦函数に対して一次の近似が開口部で成立するとすれば，等振幅線，等位相線は海岸線に平行に走る．そして開口部前面の波は，広海の進入波と同じ周期と波長をもち，水路に向つて進む．

(3) 広海における波について

広海における波は二種類の波よりなつている．すなわち定常波と減衰反射波とからである．そしてわれわれにとつて興味のあるのは後者である．

この波について次のことが知られる．

減衰反射波は，kd が小さいときは小さく，kd が大きくなるにつれて大きくなつてくる．また，この波の減衰率も kd が小さいときは小さく，大きくなるにつれて大きくなつてくる．特に河口近傍でその減衰割合は大きい．

減衰反射波の振幅によつて作られる包絡面は，kd が大きくなるにつれて一つの漸近面に近づくようである．

次に減衰反射波の方向性については，海岸にそう方向で小さく，海岸に垂直な方向になるにつれて大きくなる．換言すれば，反射波 (減衰反射波を含んで) 中で減衰反射波の占める割合は海岸に垂直な方向で最も大きい．